Electronic Supplementary Material (ESI) for ChemComm.
This journal is © The Royal Society of Chemistry 2018

TiO_2/TiN core/shell nanobelts for efficient solar hydrogen generation

Xin Yu,[a] Zhenhuan Zhao,*[b] Deihui Sun,[a] Na Ren,[a] Longhua Ding,[a] Ruiqi Yang,[a] Yanchen Ji,[a] Linlin Li[c] and Hong Liu*[ad]

[a]Institute for Advanced Interdisciplinary Research, University of Jinan, Jinan 250022, P. R. China

[b]School of Advanced Materials and Nanotechnology, Xidian University, 710071, P. R. China

[c]Beijing Institute of Nanoenergy and Nanosystems, Chinese Academy of Sciences, Beijing, 100083, P.R. China

[d]State Key Laboratory of Crystal Materials Shandong University, Jinan, 250100, P. R. China

Experimental Section

Materials

All the reagents in this work are analytic grade and commercially available. Titania P25 (TiO_2; ca. 80% anatase, and 20% rutile), sodium hydroxide (NaOH), chloroplatinic acid ($H_2PtCl_6 \cdot 6H_2O$), hydrochloric acid (HCl) and methanol (CH_3OH) were purchased from China National Medicines Corporation Ltd. All the chemicals were used as received without further purification. Deionized water was used throughout this study.

Synthesis

Synthesis of the TiO_2 nanobelts.

The synthesis of pristine anatase TiO_2 nanobelts are described in detail in our previous paper. Briefly, 0.3 g P25 were added to 70 mL of 10 M NaOH aqueous solution. The mixture was vigorously stirred for 1 h and then transferred to a 100 mL Teflon-lined stainless steel autoclave. The autoclave was sealed and put into a preheated oven to

perform hydrothermal treatment at 200 °C for 48 h. After hydrothermal processing, a white fluffy powder was collected and washed with copious amounts of deionized water and 0.1 M hydrochloric acid until the pH of the washing solution was less than 7. This resulted in the $H_2Ti_3O_7$ nanobelts. This product was then dried in an oven at 80 °C overnight. The samples were then heated in a quartz tube furnace at 800 °C for 2 h at a ramp rate of 400 °C /h. As a result, the pristine single-crystalline anatase TiO_2 nanobelts were obtained.

Synthesis of the TiN/TiO_2 core-shell nanobelts.

Subsequently, anatase TiO_2 nanobelts were heat treated in an NH_3 flow in a tubular furnace equipped with a gas flow controller. For TiN/TiO_2 samples were obtained by NH_3 directly treatment at 800 °C for 5 min using slide rail furnace.

Synthesis of the N-TiO_2 nanobelts.

The pristine sample was also annealed at 550 °C in NH_3 to from N-TiO_2 for comparison. According to the previous research by Nianqiang Wu' group[1], the nitrogen-doped TiO_2 nanobelts were prepared by heat treatment in NH_3 at elevated temperatures. The N-doped nanobelts retained the anatase structure after exposure to NH_3 form at 525 to 600 ^oC. A trend in the photocatalytic activity has been observed in the following order: N550 > N575 > N525 > pristine > N600.

Synthesis of the TiO_2/Pt nanobelts.

To enhance the hydrogen evolution ratio, TiO_2 nanobelts were loaded with 1 wt% platinum by a photo-deposition process. Briefly, TiO_2 nanobelts and $H_2PtCl_6 \cdot 6H_2O$ (c = 10 g/L) were suspended in 20:80 vol mixture of ethanol:water, and were irradiated with a Mercury lamp (300 W) for 30 min. Obtained samples were filtered and washed.

Materials characterization

XRD pattern of the samples were recorded by X-ray diffraction spectrometer with Cu Kα radiation (D8-advance, BrukerAXS, Germany). The morphology and microstructure of the samples were examined by SEM-a HITACHI S-8020 microscopy.

The TEM images were acquired on a JEOL JEM-2100 microscope with an operating voltage of 200 kV. The sample for TEM was prepared by dropping a methanol

suspension of the sample powder onto a copper microgrid. The sample was thoroughly dried in vacuum prior to observation. UV-vis diffuse reflectance spectra (DRS) of the samples were recorded on a UV-vis spectrophotometer (UV-3600, Shimadzu) with an integrating sphere attachment within the range of 200 to 800 nm and with $BaSO_4$ as the reflectance standard. The PL spectra was measured with a Horiba Jobin Yvon (FluorMax 4) Luminescence Spectrometer under a laser excitation of 375 nm. The time-resolved PL decay curve was taken out with combined steady state and time resolved fluorescence spectrometer (FLS980, Edinburgh).

The H_2 evolution experiments were carried out in a gas-closed circulation system. In a typical reaction, the 50 mg catalyst powder was dispersed in CH_3OH aqueous solution using a magnetic stirrer (70 mL of distilled water + 30 mL of CH_3OH). A commercial solar simulator (300W) equipped with a Xenon lamp as the UV-Vis light source and the Xe lamp with a cut-off filter ($\lambda > 420$ nm) was used as the visible light source for photocatalytic H_2 generation. The power density of the incident light was about 100 mW/cm^2. The H_2 evolution was measured with an on-line gas chromatograph (GC-7920).

Photoelectrode fabrication: 50 mg of photocatalyst sample was mixed with 20 mL of terpineol and stirred with a magnetic stirrer for 10 h. The suspension was dip-coated onto the uorine- doped tin oxide (FTO) glass substrate. A doctor blading technique was employed to ensure the same thickness for each photoelectrode. The photoelectrode was dried on a hot plate at 80 ^oC, and then heated in a quartz tubular furnace in Ar at 200 ^oC for 2 h. A Cu wire was connected to the FTO substrate with the silver colloid paste. Finally, epoxy was solidified to cover the FTO substrate, the silver paste and the Cu wire to avoid short current in the measurement.

Photoelectrochemical measurement: photoelectrochemical analyses were carried out using a standard three-electrode cell with Ag/AgCl as reference electrode and Pt sheet as the counter electrode in the KCl solution (1M). The electrolyte was bubbled with N_2 for 2 h to remove O_2. The light source was a 300 W Xe lamp and a cut-off filter with $\lambda > 420$ nm was also used during the measurements. The applied potential was 0.1 V vs Ag/AgCl.

In situ XPS analysis: In the present work, visible light irradiation was carried out in XPS preparation chamber, and the sample was then transferred to XPS analysis chamber without being exposed to the air. This “in situ” setting makes it possible to eliminate the influence of environmental pollutions, thereby permitting the detection of the intrinsic surface reaction under visible light irradiation. A Mercury–Xenon lamp (LC8, HAMAMATSU, 200 W, Japan) with 420 and 800 nm cutoff filters was used as an excitation light source, and introduced into the XPS preparation chamber though a sapphire window. Prior to the illumination of the sample, CH_3OH was adsorbed onto the surface of the sample by vacuum drying of the suspension. After the irradiation in XPS preparation chamber, the photoinduced holes were quenched by the photocatalytic oxidation of CH_3OH, whereas photoexcited electrons remained in sample. Thus, the differential spectrum between before and after irradiation was attributed to the electrons in sample.

The Kubelka-Munk function based on the diffuse reflectance spectra is employed to determine the band gap. For the indirect band gap semiconductor, the relation between the absorption coefficient (A) and photon energy (hν) can be written as

$$\left(\frac{Ah\nu}{K}\right)^2 = h\nu - E_g$$

Where K is absorption constants for indirect transitions, A is diffuse reflectance UV absorbance, hν = 1240/λ.

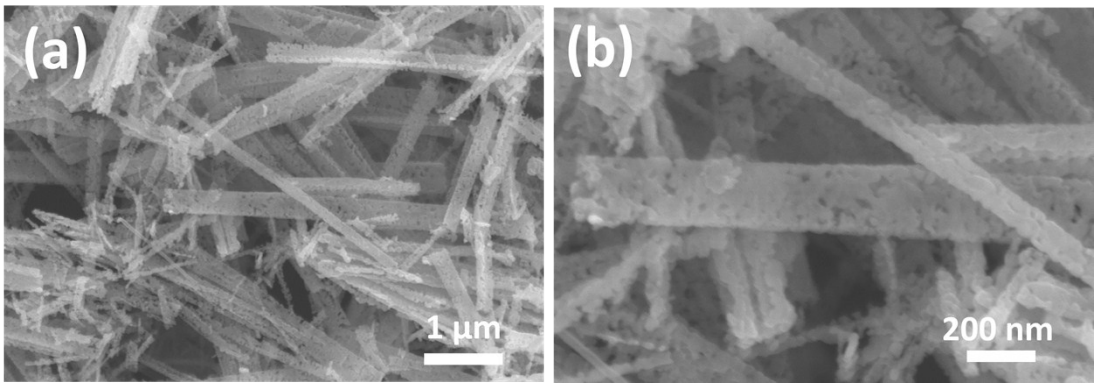

Fig. S1 SEM images of the TiN nanobelts.

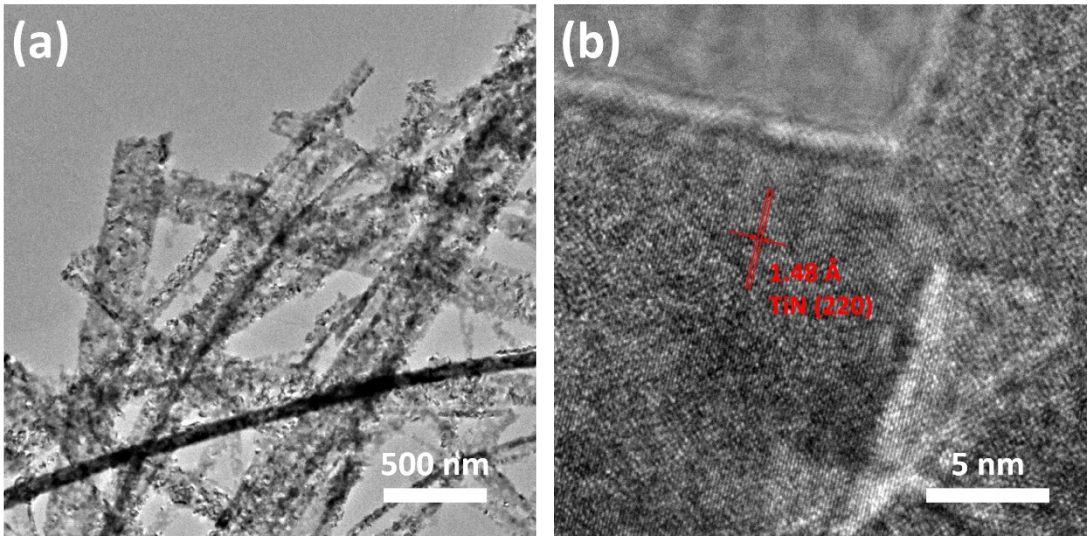

Fig. S2 (a) TEM image of TiN nanobelts and (b) HRTEM image of TiN nanobelts.

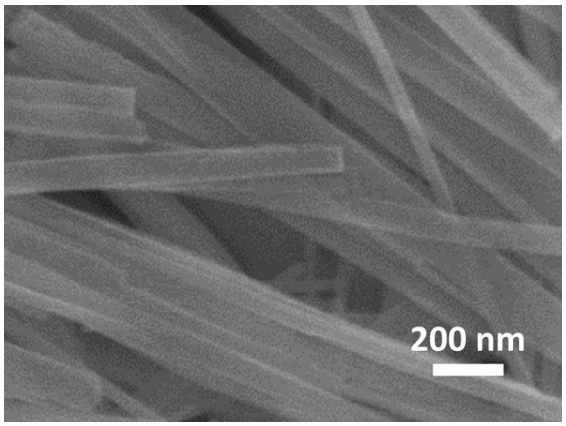

Fig. S3 SEM images of TiO_2/TiN core-shell nanobelts.

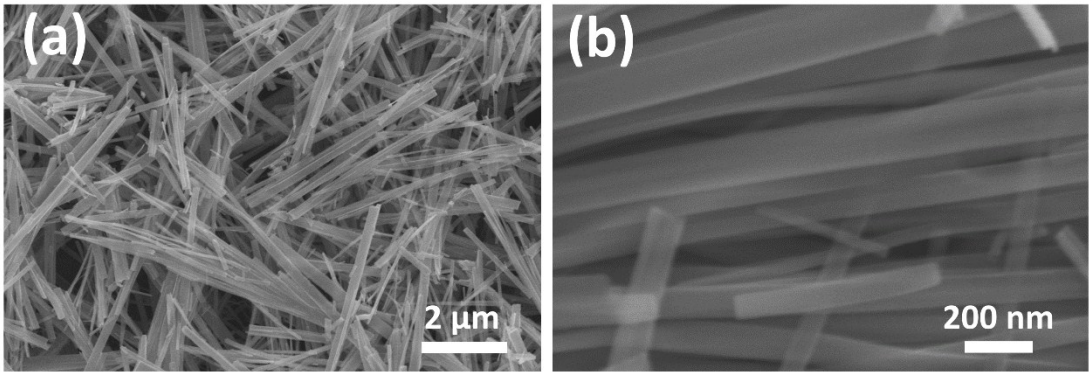

Fig. S4 SEM images of the TiO_2 nanobelts.

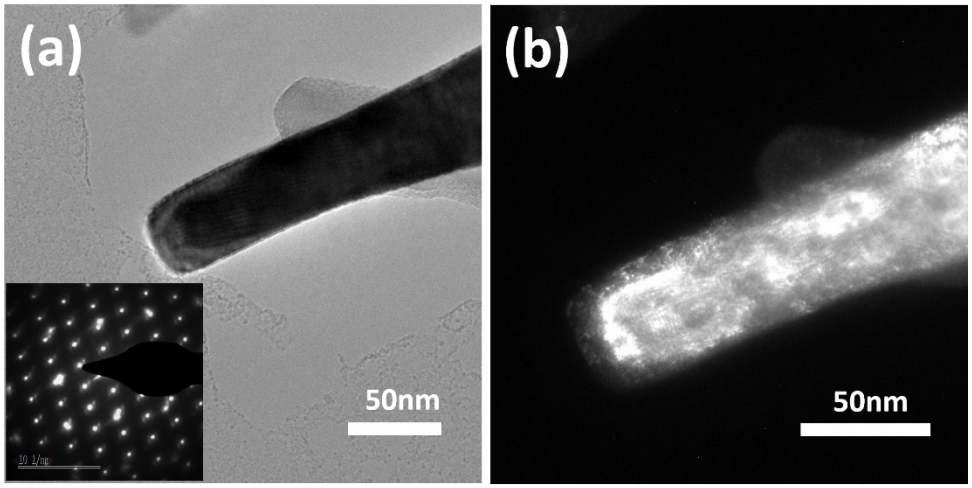

Fig. S5 TEM images of TiO_2/TiN nanobelts.

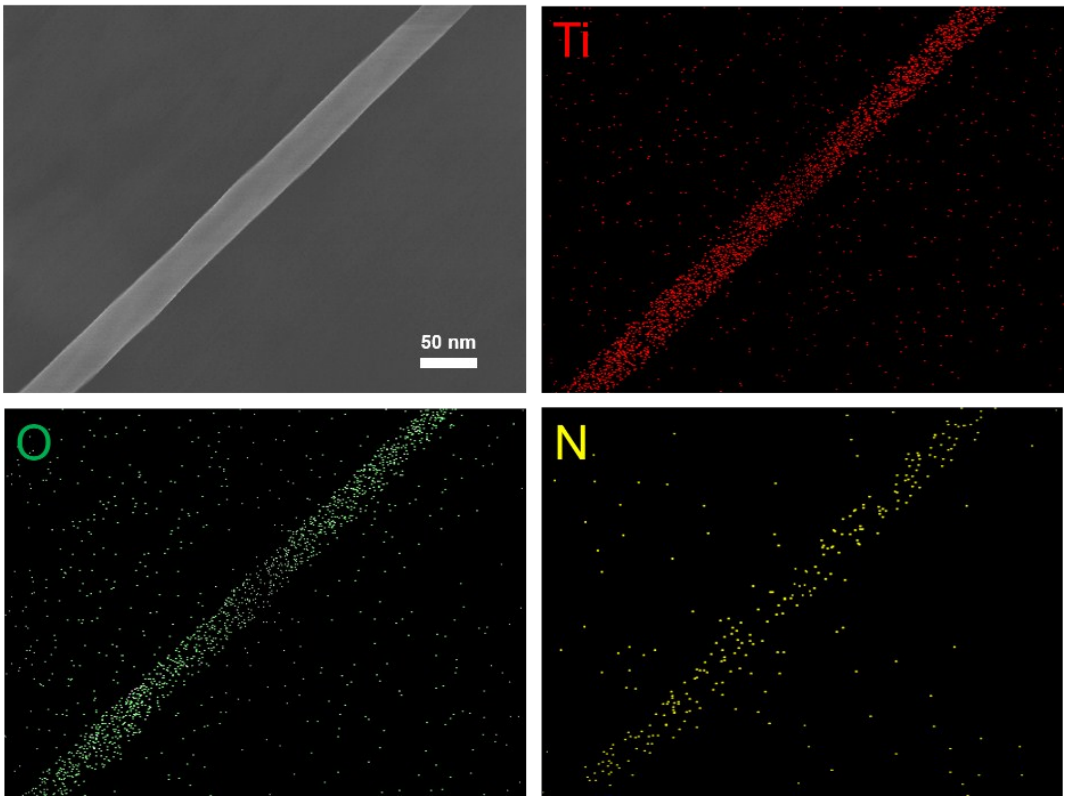

Fig. S6 EDS elemental mapping results from a single TiO_2/TiN nanobelt.

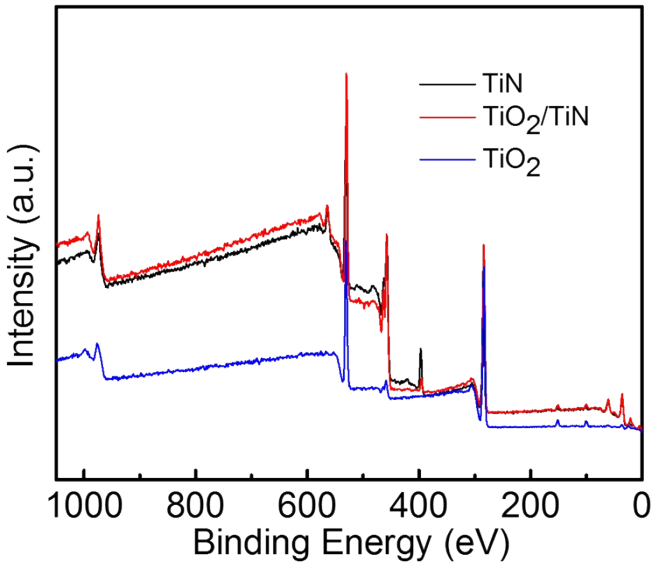

Fig. S7 XPS fully scanned spectrum of the TiN, TiO_2/TiN and TiO_2 nanobelts.

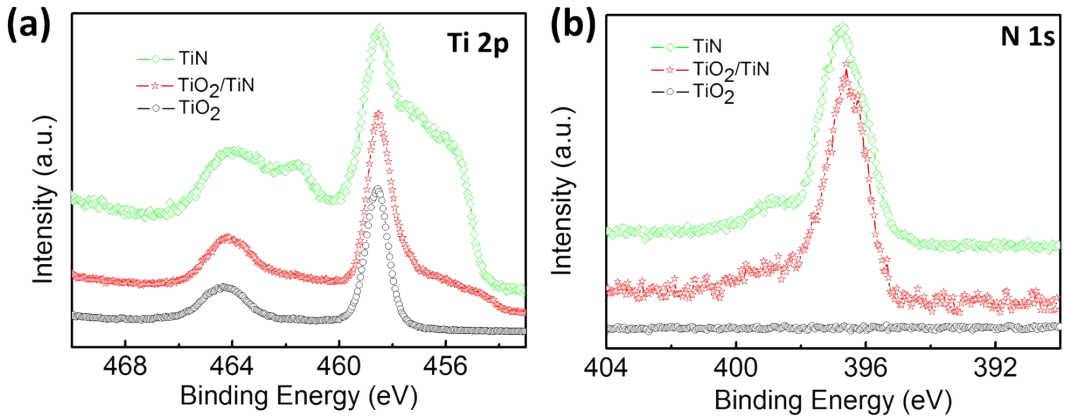

Fig. S8 XPS spectra (a) Ti 2p and (b) N 1s peaks for TiO_2, TiO_2/TiN and TiN nanobelts.

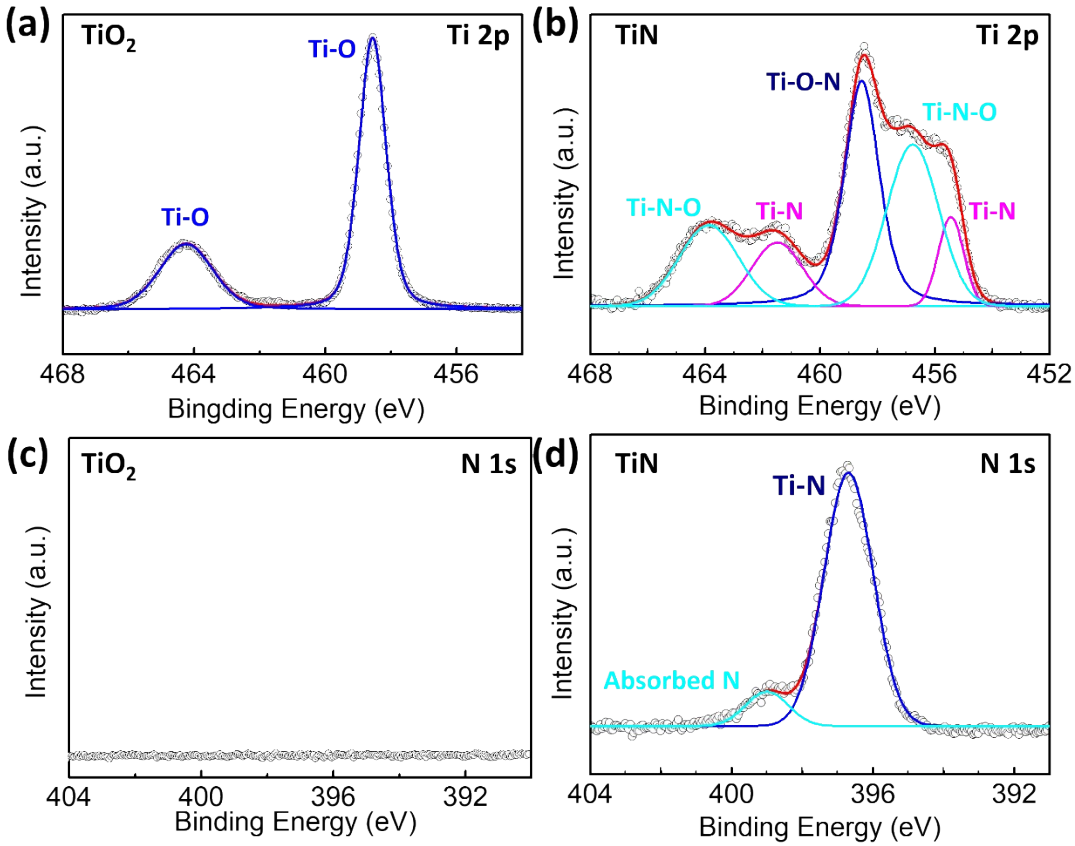

Fig. S9 Ti 2p of (a) TiO_2 and (b) TiN, and N 1s spectra of (c) TiO_2 and (d) TiN.

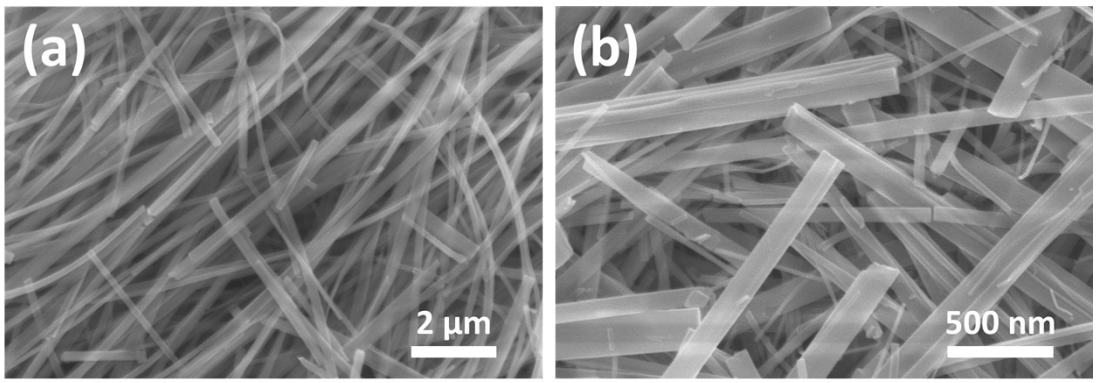

Fig. S10 SEM images of the N doped TiO_2 nanobelts.

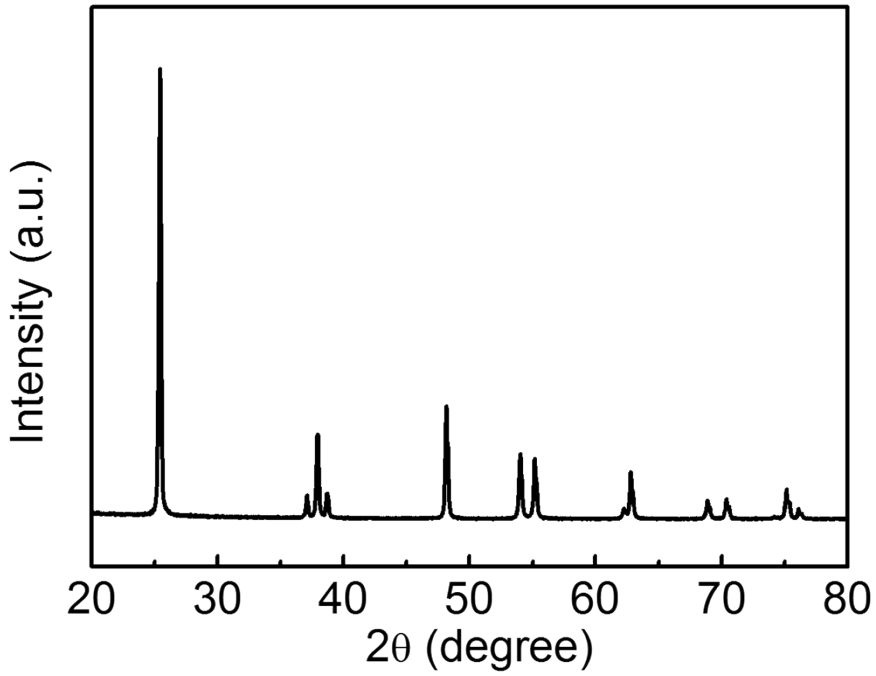

Fig. S11 XRD patterns of the N-TiO_2 nanobelts.

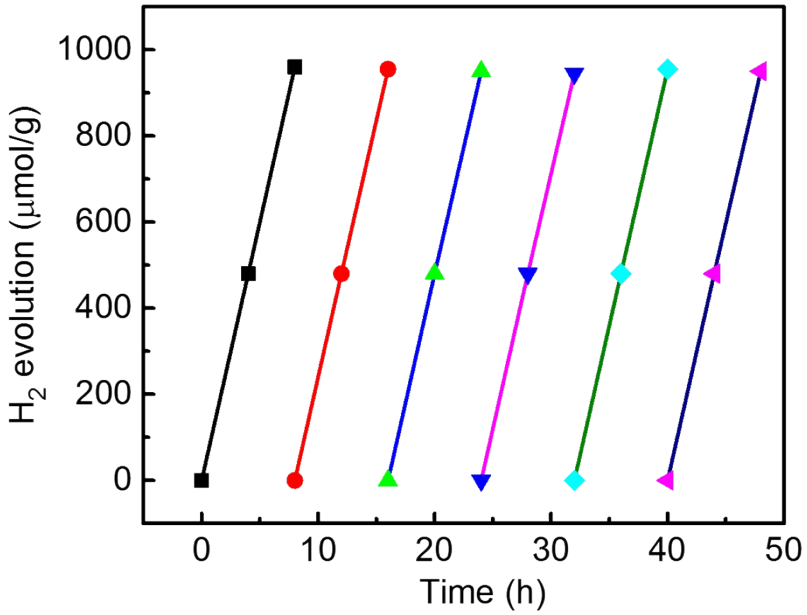

Fig. S12 Photocatalytic H_2 evolution in 6 repeated cycles (6 h/cycle) by the TiO_2/TiN nanobelts.

Table S1 Summary of the photoluminescence decay time (τ) and their relative amplitude (f) in the samples, which are derived from the time-resolved PL spectra in Fig. 4b by biexponential decays

Sample	Decay time [ns]		Relative amplitude [%]		Average lifetime [ns]
	τ_1	τ_2	f_1	f_2	τ^a
TiO_2 NBs	1.28	18.06	48.90	51.10	20.84
TiO_2/TiN NBs	1.97	33.37	5.12	94.88	36.49

[a]The average lifetime was calculated using equation: $<\tau_1> = (f_1\tau_1^2 + f_2\tau_2^2)/(f_1\tau_1 + f_2\tau_2)$.